Semiconductor Physics, Quantum Electronics & Optoelectronics, 2020. V. 23, No 4. P. 346-354.

Semiconductor physics

Characterization of nano-bio silicon carbide

S.I. Vlaskina[1], G.N. Mishinova[2], I.L. Shaginyan[3], P.S. Smertenko[4], G.S. Svechnikov[5]

[1]Yeoju Institute of Technology (Yeoju University),
338, Sejong-ro, Yeoju-eup, Yeoju-gun, Gyeonggi-do, 469-705 Korea,
E-mail: businkaa@mail.ru or svitlanavlaskina1949@gmail.com
[2]Taras Shevchenko Kyiv National University, 64, Volodymyrs'ka str., 01033 Kyiv, Ukraine
[3]Seoul National University SNUSD, 101 Daehak-ro, Jongno-gu, Seoul 03080, Korea
[4]V. Lashkaryov Institute of Semiconductor Physics, NAS of Ukraine,
41, prospect Nauky, 03680 Kyiv, Ukraine
[5]National Technical University of Ukraine "Igor Sikorsky Kyiv Polytechnic Institute",
37, Peremohy Ave., Kyiv, Ukraine

Abstract. Plasma-enhanced chemical vapor deposition, reactive magnetron sputtering, hot-wire chemical vapor deposition and radio frequency plasma-enhanced chemical vapor deposition were used to develop technology for preparation of nano-bio silicon carbide coating of ceramic materials for dental applications. The effect of the bias voltage applied to the ceramic prostheses and dental crowns on the crystallization processes have been recognized. The optimal bias voltage applied to conductive substrate was –200 V, whereas for dielectric substrate the bias voltage V_{bias} did not affect the properties of SiC coating. The analysis of CVCs and spectroscopic diagnostics as the methods for studying the mechanism of interfacial rearrangements to investigate SiC phase transition in nano silicon carbide coatings were used. The conductivity of the SiC coating coincided with the conductivity on the dielectric ($\mu n_0 = 10^{12}\ldots10^{13}$ cm$^{-1}\cdot$s$^{-1}\cdot$V^{-1}). The conductive substrate had a significant effect on the properties of the coating and thus depended on the bias voltage V_{bias}. The conductivity increased by three-four orders of magnitude ($\mu n_0 = 3\cdot10^{17}$ cm$^{-1}\cdot$s$^{-1}\cdot$V^{-1}), if the bias voltage $V_{bias} = -200$ V. The increase of the bias voltage ($V_{bias} = -600$ V) led to a decrease in the conductivity ($\mu n_0 = 10^{11}\ldots10^{12}$ cm$^{-1}\cdot$s$^{-1}\cdot$V^{-1}). It was found that there was the double injection regime with bimolecular recombination in this structure with the dependence $I = V^{3/2}$ for CVCs of SiC. The luminescence spectrum of SiC coating on non-dielectric ceramics (if $V_{bias} = -200$ V during deposition) was significantly different from the luminescence spectrum of SiC coating on dielectric ceramics. Increasing the applied voltage to the substrate V_{bias} during deposition led to increasing the fraction of hexagonal polytypes. Directions in the crystal lattice according to the photoluminescence spectra were identified from the comparing the values of the width of the non-phonon parts of stacking faults and deep level spectra in the low-temperature photoluminescence with arrangements of atoms in the SiC lattice structure. The displacement of each atom participating in photoluminescence allowed to find the correlation with technology of SiC deposition and to develop technology of SiC coating on the dental materials.

Keywords: silicon carbide, nanosilicon carbide, bio-based ceramics, current-voltage characteristic, photoluminescence, dental application.

https://doi.org/10.15407/spqeo23.04.346
PACS 78.55.-m, 81.15.Cd, 81.15.Gh, 81.15.-z, 81.05.Je, 81.05.Mh, 84.37.+q, 87.85.jj

Manuscript received 07.09.20; revised version received 12.10.20; accepted for publication 28.10.20; published online 19.11.20.

1. Introduction

Silicon carbide is extremely inert material, that is why the development of bio-based SiC ceramic technology is very important today for bio and medical applications [1-4]. Analysis of the erosive effect of different substance and medications has shown that different pH levels affect the surface of dental ceramics. Ceramic corrosion can start by all kinds of acidic drinks (Coca Cola: pH = 2.45, Red Bull: pH = 3.17, wines: pH = 3.74), food (beef: pH = 4.1…7.0), fruits (grapefruits: pH = 3.3), vegetables (spinach and soybeans: pH = 8…14) and so on. SiC is a promising ceramic material for medical applications, since SiC has such properties as high strength, corrosion

resistance [5, 6]. SiC demonstrates excellent biocompatibility as well (higher biocompatibility than silicon [7]). As a dental material SiC coating displayed adjustable color to match the dental shade guide used in clinic and wear resistance [8]. Another possible biocompatible material is nano-SiC reinforced Zn biocomposite. Zn has been regarded as a potential implant biomaterial due to the good biocompatibility, but the low strength and ductility limit of its application. Nano-SiC, incorporated into Zn matrix, improves the mechanical performance and biocompatibility. Biocomposites were prepared *via* laser melting [9].

Silicon carbide biotechnology provides biocompatible and long-term *in vivo* application ranging from heart stent coatings and bone implant to neurological implants and sensors [10]. The main problem facing the medical community is the lack of biocompatible material that is also capable of electronic operation. Such devices are currently implemented using silicon technology, which has to be hermetically sealed so it cannot interact with the body. Silicon as material is stable *in vivo* for short period of time only. Silicon carbide has been proven as a material for long term use (permanent implanted devices, namely: glucose sensors, brain machine interface devices, smart bone, organ implants) [11, 12]. The body does not recognize SiC and does not reject as a foreign (*i.e*., inorganic) material. The use of SiC opens up the development of advanced biomedical devices for long term use *in vivo* [13]. As an indirect-bandgap semiconductor, bulk SiC has week luminescence, but porous SiC and SiC nanocrystals show bright photoluminescence [14].

One of the most basic directions in solid state physics is the study of formation of various crystalline phases in single crystals, in thin films, in powders, and in nanocrystals. The various crystalline phases (polytypes) are formed at the same thermodynamic growth parameters (temperature, pressure, impurity concentration). Moreover, the phase transformations are observed at the slightest occurrence of violations of the crystal structure, transitions of some polytypic phases to others. This phenomenon is typical for metals, semiconductors, ceramics, organic compounds and manifests itself both in bulk materials and in thin-film and nanomaterials, both in single crystals and in polycrystals, both in layered and in close-packed structures of C, Si, SiC, ZnS, CdS, AlN, BN, *etc*. [15-18]. Moreover, polytypism does not depend on the type of bonds. Both for substances with a diamond-like crystal lattice with a predominantly covalent type of bond, and for substances with a hexagonal lattice such as graphite (covalent bonds in layers and van der Waals bonds between layers), one can apply the same model and consider different structures as equivalent consisting of close-packed spheres of equal diameter. Ascertaining general patterns of formation and transitions of polytypes makes it possible to find the reasons for formation of polytype modifications in various compounds [17, 19].

If we consider a three-dimensional close packing of atoms and designate the first layer as type A, the next layers will be densely arranged in positions of type B or type C. Neighboring layers in close packing cannot be of the same type. The polytypes differ in the order of alternation and the repetition period in the direction of the crystallographic axis and the type of unit cell. So, for ABABABAB packing, the recurrence period of the layers is 2 and the unit cell is hexagonal (h), the designation is 2H polytype; and for ABCABCA the recurrence period is 3, the unit cell belongs to the cubic (C) system, the designation of the polytype is 3C. One of the brightest representatives of polytype materials is silicon carbide SiC.

All silicon carbide polytypes fundamentally differ only in the number and sequence of packing of dense atomic Si-C bilayers in a cubic (ABC) or hexagonal (AB) position relative to adjacent (neighboring) bilayers. Then the replacement of any layer in the cubic setup with the hexagonal one (or vice versa) can be considered as a stacking fault (SF) of the given polytype. Accordingly, in the hexagonal polytypes in the $(11\bar{2}0)$ plane, there is a strictly defined alternation of atomic layers along the [0001] axis. They are called zig-zag chains in the plane $(11\bar{2}0)$. Similarly, by the regular introduction of the stalking faults SF packing defects (that is, hexagonal h layers) into the cubic 3C-SiC structure (β-phase) along one of the directions of dense packing of ⟨111⟩ layers, one can obtain any hexagonal (H) or rhombohedral (R) structure α-phases.

Therefore, polytypes have varying degrees of hexagonality, *i.e*., the fraction of the number of hexagonal layers of layers relative to the total number of layers in the unit cell of the polytype. A hexagonal layer is the layer in which adjacent layers have the same designations – in the ABA sequence, layer B is hexagonal (h). In the ABC sequence, layer B is not hexagonal, but cubic (c) [20].

Thus, the structural, optical and electro-physical properties of polytypes of the same material are defined by this degree of hexagonality. For example, if we study the low-temperature luminescence spectra of SiC with stacking faults (SF) and consider the energy position of the short-wave edge of the phononless part of each stacking fault, as well as the positions of the corresponding excitation spectra, then they linearly depend on the percentage of hexagonality [21]. This makes it possible to determine with high accuracy the band gap of both stable and metastable polytypes [22]. It also allows one to record the process of phase transformation through formation of certain structures [23].

The goals of this work are as follows: (i) to develop technology of coating of ceramic materials with silicon carbide for dental applications; (ii) to perform characterization of this coating in comparison with monocrystalline SiC; (iii) to study mechanisms of interfacial rearrangements to investigate SiC phase transition in nano-silicon carbide both as-grown and that occurring

under deformation; (iv) to analyze the structure and regularities of formation and transformation of polytype structures in nano-silicon carbide by their electro-physical optical properties for a possible their correlation with technology of bio-silicon carbide deposition. This correlation can be used to develop further technology for medical doctors and practitioners, who are ready to identify and implement advanced engineering solution to their everyday medical practice.

2. Experimental

The SiC coatings were deposited on ceramic prostheses and dental crowns by thermal decomposition of methyl-thrychloro-silane CH_3SiCl_3 molecules by using the plasma-enhanced chemical vapor deposition (PECVD) process. C and Si atoms were extracted from the plasma on the substrates by the electrical field using the bias voltage V_{bias} applied to the substrates. The presence of an electrical field led to a localized drift of charged particles (electrons and ions) near the substrate surface. This way increased the lifetime of incoming particles and led to the intensification of the deposition process. Different configurations of upper electrode allowed to control deposition of all parts of prostheses and crowns. The bias voltage V_{bias} was varied from –100 V up to –600 V. Control depositions were made on Si, Al_2O_3, AlN and glass substrates. The temperature of substrate did not exceed 200 °C. Before the deposition, the vacuum chamber and substrates were cleaned with hydrogen. Later hydrogen served as a gas carrier and delivered CH_3SiCl_3 to the RF discharge field. This deposition technique made it possible to coat substrates of any configuration at low temperature.

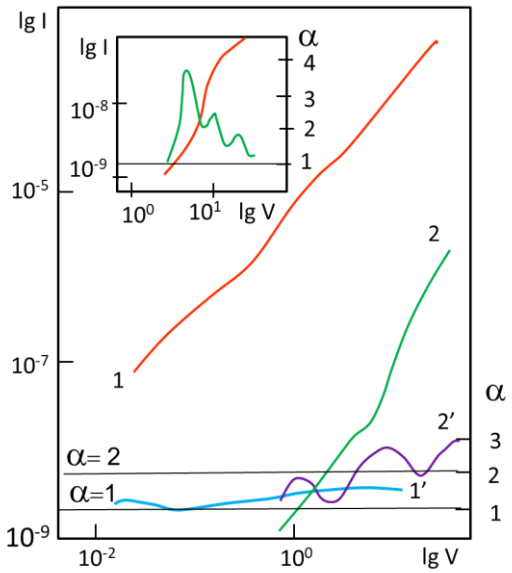

Fig. 1. CVCs (*1*–*3*) and their dimensionless sensitivity α (curves *1'*–*3'*) of SiC films on Si at different bias voltage V_{bias}: V_{bias} = 0 (*1*) and V_{bias} = –200 V (*2*); on insert the glass is substrate.

Plasma-enhanced chemical vapor deposition (PECVD), reactive magnetron sputtering, hot-wire chemical vapor deposition (HW-CVD) and radio-frequency plasma-enhanced chemical vapor deposition (RF-PECVD), very high frequency plasma-enhanced chemical vapor deposition (VHF-PECVD) [24] were also used for the SiC coatings because of lower operation temperature as compared to the physical methods (physical vapor transport) or sublimation.

Deposited compositions were investigated using the Auger analysis and corresponded to stoichiometric SiC. Surface morphology, as followed from electron microscopy data, were smooth and uniform.

The analysis of current-voltage characteristics (CVCs) and spectroscopic diagnostics were used for studying the mechanisms of interfacial rearrangements, for investigation of SiC phase transition in nano-silicon carbide both as-grown and occurring under deformation. Results of this electro-physical and spectroscopic diagnostics allowed to find correlation between parameters of deposition technology and peculiarities of coatings structure. The analysis of CVCs was based on dimensionless sensitivity approach [25, 26], where the dimensionless sensitivity is determined as $\alpha = d\lg I / d\lg V$.

Low temperature spectra were obtained by excitation of nitrogen, He-Cd, Ar-lasers and mercury and xenon lamps. The PL spectra were measured using the samples contained in a liquid helium or nitrogen cryostat, which provided the temperature range from 1.5 up to 330 K.

3. Results and discussions

SiC was simultaneously coated on conductive and dielectric substrates of metal, silicon, glass and sapphire. CVCs and their dimensionless sensitivity α are shown in Fig. 1. Within the low voltage range ($V = 10^{-2}…10^{-1}$ V), α is close to unity. It is indicative of the dominant role of the bulk in the resistance of the deposited film. The conductivity of the SiC coating coincides with that on the dielectric ($\mu n_0 = 10^{12}…10^{13}$ cm^{-1}·s^{-1}·V^{-1}). The conductive substrate has a significant effect on the properties of the coating, which depends on the bias voltage V_{bias}. The conductivity increases by three-four

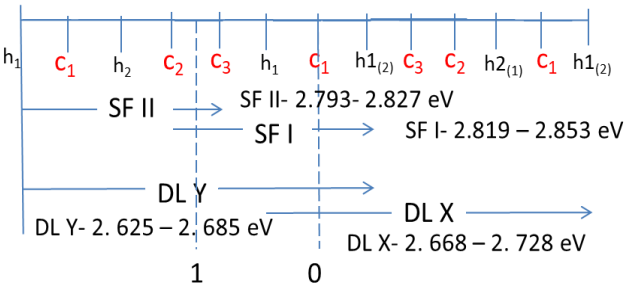

Fig. 2. The energy scale of the photoluminescence, the hexagonal (h) and the cubic (c) positions of atoms (according the data in Table).

orders of magnitude ($\mu n_0 = 3 \cdot 10^{17}$ cm$^{-1}\cdot$s$^{-1}\cdot$V^{-1}), if the bias voltage $V_{bias} = -200$ V. The increase of the bias voltage ($V_{bias} = -600$ V) leads to a decrease in the conductivity ($\mu n_0 = 10^{11}\ldots10^{12}$ cm$^{-1}\cdot$s$^{-1}\cdot$V^{-1}).

Consequently, if the prosthesis ceramic is dielectric, then the bias voltage V_{bias} does not affect the properties of SiC coating. If the prosthesis ceramic is not dielectric, then elimination of intergranular defects is observed due to the presents electrical of a pulling field. Further increasing the bias voltage V_{bias} leads to breaking the SiC coating and to the conductivity decrease.

CVCs have the distinguished jump of current ($\alpha_{max} = 3.27$, if the prosthesis ceramic is not dielectric and $\alpha_{max} = 3.83$, if the prosthesis ceramic is dielectric) as well as the range where $I \sim V^{3/2}$. The current jump is described by the regime of significant injection of current carriers from the contacts (observed only in the case, if the prosthesis ceramic is dielectric, or if $V_{bias} = 0$ on the non-dielectric prosthesis ceramic). The discrimination coefficient ($Q_m = 10^{-4} << 1$) is typical for double injection. This is evidence of high conductivity and high recombination of charge carriers, what is very important for quick discharge of any charge at the interface with SiC substrate. The calculated values of n_{max} (at the extremum point) and lifetime τ_{pm} are close to the corresponding values of nanocrystalline SiC. The carrier capture coefficient is $\gamma_0 = 2.8 \cdot 10^{-11}$ s$^{-1}\cdot$cm^{-1}. The dependence $I = V^{3/2}$ confirms the double injection regime with bimolecular recombination in this structure.

So, based on the study of the electro-physical parameters of the SiC coatings, it can be concluded that the deposited coatings are nanocrystalline.

The luminescent analysis is one of the well-developed research methods in biology and therapy. The luminescence spectrum of SiC coating on non-dielectric ceramics (if $V_{bias} = -200$ V during deposition) significantly differs from the luminescence spectrum of SiC coating on non-dielectric ceramics in the case when $V_{bias} = 0$ during deposition. Namely, the shift of photo-luminescence maximum to shorter wavelengths is observed. The appearance of the structure and the shape of the spectrum characteristic of hexagonal SiC is observed, too.

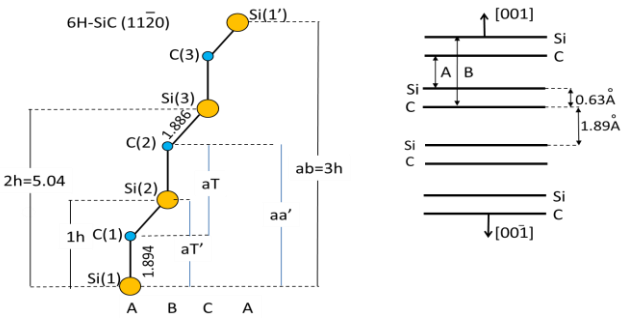

Fig. 3. Lattice structure of SiC: a) position of Si and C atoms in the (11$\bar{2}$0); b) schematic diagram of SiC showing the sequence of Si-C double layers and the definition of the [001] axis.

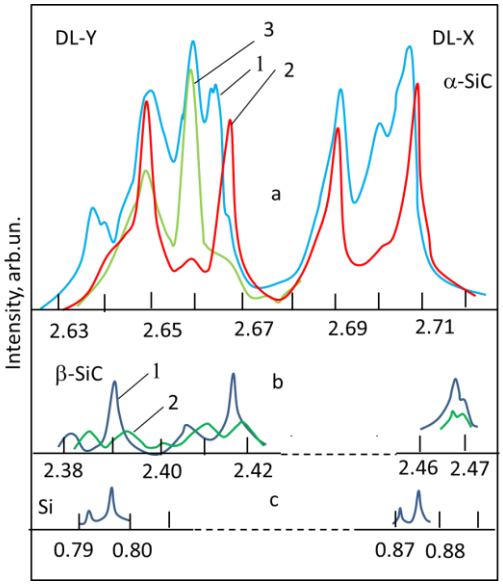

Fig. 4. Zero-phonon parts of the DL spectra in SiC and Si: a) *1* is sample N1$_{DL}$, *2* is N2$_{DL}$, *3* is N6$_{DL}$; b) *1* is N2$_{\beta}$ as grown joint polytypes, *2* is N9$_{\beta}$ in the zone of maximum deformation by bending at $T = 210$ °C for 30 min; c) Si sample. From Ref. [27].

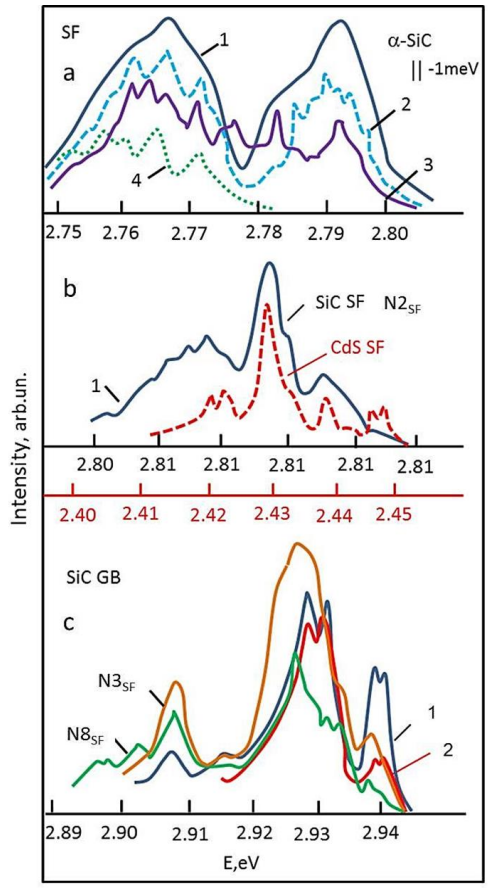

Fig. 5. Zero-phonon parts of SF and GB spectra: a) zero-phonon parts of the SF spectra in SiC, calculated by the translation of the TA phonon; b) zero-phonon parts of the SF spectra in SiC and in CdS, actually manifested; c) zero-phonon parts in the GB spectra actually manifested. From Ref. [27].

N	Spectrum parameters, energy scale, meV	Spectrum parameter, symbol	Tetrahedral parameter		Angular scale, degree
			Å	symbol	
1	4.3		0.315		9
2	8.6	overlap SFI and SFII, TT′	0.63	distance in layer SiC between Si and C atoms	18
3	12.9		0.945		27
4	17.2		1.26		36
5	21.5		1.575		45
6	25.8	shift between the centers SFI and SFII	1.89	distance between C atom in the first layer and Si atom in the next layer	54
7	30.1		2.205		63
8	34.4	aT, a′T′ or SFI and SFII	2.52	height of tetrahedron, h	72
9	38.7		2.835		81
10	43	shift between the centers of DLX and DLY	3.15	rotation DLX and DLY	90
11	47.3		3.465		99
12	51.6		3.78		108
13	55.9		4.095		117
14	60.2	aa′, DLY, or DLX, or SF = SFI + SFII	4.41		126
15	64.5		4.725		135
16	68.8		5.04	2h	144
17	73.1		5.355		153
18	77.4		5.67		162
19	81.7		5.985		171
20	86		6.3		180
21	90.3		6.615		189
22	94.6		6.93		198
23	98.9		7.245		207
24	103.2	DL = DLX + DLY, ab	7.56	3h	216

Hence, the photoluminescence spectrum of the SiC coating on non-dielectric ceramics (V_{bias} = –200 V) indicates that the coating contains nanoinclusions of both the cubic polytype and hexagonal polytypes. The increase of the voltage V_{bias} applied to the substrate during deposition leads to the increase in the fraction of hexagonal polytypes. This change in the photoluminescence spectra of the coatings in the absence of bombardment of the substrate with plasma ions (V_{bias} = 0) and in the presence of bombardment (V_{bias} = –200 V) indicates that the processes of nanocrystallization occur on the surface of the substrate and are defined by the energy of bombarding ions coming from the plasma.

There are three types of photoluminescence spectra: stalking faults (SF), deep levels (DL) and grain boundaries (GB). SF and DL reflect the fundamental logic of

SiC polytypes [27]. From analysis of SF [20] and DL [28] spectra, it follows that the spectra can reflect the positions of atoms. SiC has several different polytypes according to the stacking sequence of SiC atomic double layers in the crystal lattice. The difference in number and sequence of atomic layers packing in cubic (ABCABC) or hexagonal (ABAB) SiC leads to different SiC polytype growth. Determination of cubic SiC structure or the hexagonal SiC has shown that all properties of different polytypes strongly depend on defects. If nanocrystal has dimension below 1 nm, then only one crystal structure can exist. The bigger nanocrystals (1 to 3 nm and larger) can exist in the form of cubic and hexagonal polytypes. The photoluminescence spectra of SiC nanocrystals are very structured.

All SF spectra have the same spectral range equal 60.2 meV and have two parts SFI (equal to 34.4 meV) and SFII (equal to 34.4 meV). The range of overlapping is equal to 8.6 meV, and mutual shift – 25.8 meV. Fig. 2 shows the energy scale of the SF spectra photoluminescence and two parts of SF: SFI and SFII.

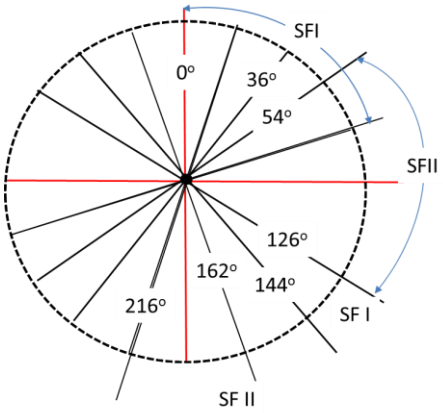

Fig. 6. Energy scale for the SFI and SFII in luminescence spectra corresponding to their angles between atoms.

All DL spectra have the same spectral range (equal to 103.2 meV) and have two parts DLX (equal to 60.2 meV) and DLY (equal to 60.2 meV). The range of overlapping is equal to 17.2 meV, and mutual shift – 43 meV. The energy range of every DLX and DLY are the same as the energy range of SF or GB. Fig. 2 shows the energy scale of the DL photoluminescence and two parts of DL: DLX and DLY.

Comparing the values of the width of the non-phonon SF and DL in Fig. 2 spectra with arrangements of atoms in the SiC structure in Fig. 3a, it is easy to see that SF should be considered in two tetrahedron, while DL are in three tetrahedron.

Therefore, the corresponding atomic position (cubic or hexagonal) on the energy scale of photoluminescence spectra can be determined. Shown in Fig. 2 are the energy scale of photoluminescence, the hexagonal (h) and the cubic (c) positions of atoms. In Fig. 3a, the positions of Si and C atoms in the $(11\bar{2}0)$ plane are shown. The sequence of Si-C double layers is shown in Fig. 3b. The complex picture of the DL spectra [27, 28] (Fig. 4) is played out within three heights inserted into each other of silicon and carbon tetrahedrons.

The complex picture of the SF spectra (Fig. 5) [20, 27, 29] is played out within two heights inserted into each other silicon and carbon tetrahedrons.

Fig. 6 shows the correspondence of the energy scale SFI and SFII in luminescence spectra to their angles between atoms. The shift between the centers SFI and SFII is equal to 25.8 meV (Table) in spectra corresponds to 54 degrees. The shift between the centers DLX and DLY in spectra is equal to 43 meV (Table) corresponds to 90 degrees. Polarization measurements showed that configuration DLX and configuration DLY were rotated 90 degrees relative to each other. It is clear that in this way the directions in the crystal lattice are easily identified (Fig. 7).

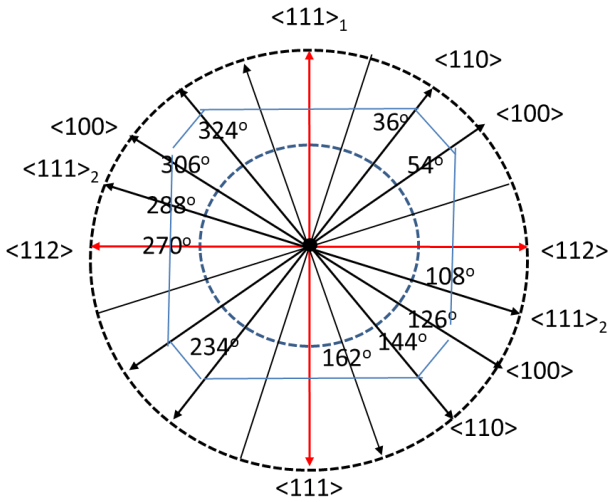

Fig. 7. Directions in the crystal lattice.

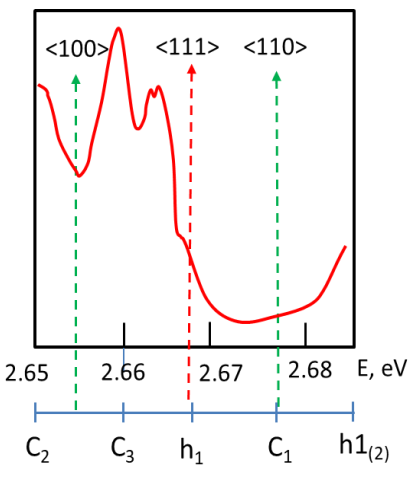

Fig. 8. Basic elements and fragments of fine structure DL spectra.

The displacement of every atom involved in photoluminescence can be seen (Fig. 8).

Therefore, SF and DL photoluminescence spectra give evidence of formation of SiC nanocrystals.

Thus, formation of nanocrystals demonstrates the effectiveness of plasma design in achieving full CH_3SiCl_3 dissociation. The presence of electrical field (V_{bias}) leads to initial nucleation, growth and crystallization involving interaction with charged species, *i.e*. ions and hot electrons. Crystallization takes place due to ion and electron bombardment during the coating process and SiC growth. Efficient photoluminescence was observed after reducing the nanocrystals size less than 1.5 nm, which is attractive for bio and medical applications.

4. Conclusions

Technology for coating the ceramic materials for dental applications have been developed on the base of plasma-enhanced chemical vapor deposition, reactive magnetron sputtering, hot-wire chemical vapor deposition and radio-frequency plasma-enhanced chemical vapor deposition. The effect of electrical field applied to the ceramic prostheses and dental crowns on the crystallization processes have been recognized. The optimal bias voltage, applied to the conductive substrate, is –200 V, whereas for dielectric substrate the bias voltage V_{bias} does not affect the properties of SiC coating. Hereby, it was found that the deposited coatings are nanocrystalline.

The analysis of CVCs and spectroscopic diagnostics as the methods for studying the mechanism of interfacial rearrangements to investigate SiC phase transition in nano-silicon carbide coatings were used. The conductivity of the SiC-coating coincides with the conductivity on the dielectric ($\mu n_0 = 10^{12}…10^{13}$ cm$^{-1}\cdot$s$^{-1}\cdot$V^{-1}). The conductive substrate has a significant effect on the properties of the coating, which depends on the bias voltage V_{bias}. The conductivity increases by three-four orders of magnitude ($\mu n_0 = 3\cdot10^{17}$ cm$^{-1}\cdot$s$^{-1}\cdot$V^{-1}), if the bias voltage $V_{bias} =$ 200 V. The increase of the bias voltage (V_{bias} = 600 V) leads to a decrease in the conductivity ($\mu n_0 = 10^{11}…10^{12}$ cm$^{-1}\cdot$s$^{-1}\cdot$V^{-1}). It was found that there is the double injection regime with bimolecular recombination in this structure with the dependence $I = V^{3/2}$ for CVCs of SiC coating at $V_{bias} = 0$.

The luminescence spectrum of SiC coating on non-dielectric ceramics (if $V_{bias} =$ –200 V during deposition) significantly differs from the luminescence spectrum of SiC coating on dielectric ceramics. The increasing of the applied to the substrate voltage V_{bias} during deposition leads to an increasing in the fraction of hexagonal polytypes.

Comparing the values of the width of the non-phonon parts of stacking faults and deep level spectra in the low-temperature photoluminescence with arrangements of atoms in the SiC lattice structure, the corresponding atomic position (cubic or hexagonal) was determined, and the directions in the crystal lattice according to the photoluminescence spectra were identified. The displacement of each atom participating in photoluminescence can be seen. It allows us to find the correlation in technology of SiC deposition and to develop technology of SiC deposition onto the dental materials. The photoluminescence was observed and analyzed after reducing the SiC nanocrystals size less than 1.5 nm which is attractive for bio and medical applications.

The analysis of CVCs and spectroscopic diagnostics allowed us to develop the method for coating the ceramic materials with silicon carbide for dental applications and to perform characterization of these coatings in comparison with single crystalline SiC. The mechanisms of interfacial rearrangements to investigate SiC phase transition in nano-silicon carbide both as-grown and that occurring under deformation have been studied. The analysis of structure and regularities of formation and transformation of polytype structures in nano-silicon carbide by their electro-physical and optical properties for a possible their correlation with technology of bio-silicon carbide deposition has been made. Technology has been developed for medical doctors and practitioners, who are ready to identify and implement the advanced engineering solution to their everyday medical practice.

References

1. Hsu Sh.-M., Ren F., Chen Zh. *et al*. Novel coating to minimise corrosion of glass-ceramics for dental applications. *Materials*. 2020. **13**, No 5. P. 1215. https://doi.org/10.3390/ma13051215.
2. Fürst Ch., Plank B., Senck S. *et al*. Bio-based silicon carbide ceramics from extruded thermoset-based wood polimer composites. *ECCM18 – 18th European Conference on Composite Materials*, Athens, Greece, June 24-28, 2018. P. 1–7.
3. Gryshkov O., Klyui N.I., Temchenko V.P. *et al*. Porous biomorphic silicon carbide ceramics coated with hydroxyapatite as prospective materials for bone implants. *Mater. Sci. Eng. C*. 2016. **68**. P. 143–152. https://doi.org/10.1016/j.msec.2016.05.113.
4. Ponraj J.S., Dhanabalan S.Ch., Attolini G., Salviati G. SiC nanostructures toward biomedical applications and its future challenges. *Critical Reviews in Solid State and Material Science*. 2016. **41**, No 5. P. 430–446. https://doi.org/10.1080/10408436.2016.1150806.
5. Cappi B., Neuss S., Salber J., Telle R., Knüchel R., Fischer H. Cytocompatibility of high strength non-oxide ceramics. *Journal of Biomedical Material Research*. 2010. **93A**, No 1. P. 67–76. https://doi.org/10.1002/jbm.a.32527.
6. González P., Borrajo J.P., Serra J. *et al*. Extensive studies on biomorphic SiC ceramics properties for medical applications. *Key Engineering Materials*. 2003. **254–256**. P. 1029–1032. https://doi.org/10.4028/www.scientific.net/kem.254-256.1029.

7. Bohaventura G., Iemmolo R., La Cognata V. *et al*. Biocompatibility between silicon or silicon carbide surface and neural stem cells. *Sci. Rep*. 2019. **9**. P. 11540. https://doi.org/10.1038/s41598-019-48041-3.
8. Chen Z., Fares C., Elhassani R. *et al*. Demonstration of SiO_2/SiC-based protective coating for dental ceramic prostheses. *J. Am. Ceram. Soc*. 2019. **102**, No 11. P. 6591–6599. https://doi.org/10.1111/jace.16525.
9. Chengde Gao, Meng Yao, Cijun Shuai, Shuping Peng, Youwen Deng. Nano-SiC reinforced Zn bio-composites prepared *via* lazer melting: Microstructure, mechanical properties and biodegradability. *Journal of Material Science & Technology*. 2019. **35**, No 11. P. 2608–2617. https://doi.org/10.1016/j.jmst.2019.06.010.
10. Schettini N., Jaroszeski M.J., West L., Saddow S.E. Hemocompatibility assessment of 3C-SiC for cardiovascular applications. In: *Silicon Carbide Biotechnology*. Ed. S. Saddow. Elsevier, 2012. P. 153–208. https://doi.org/10.1016/B978-0-12-385906-8.00005-2.
11. Cespedes F.A., Mamcu G., Saddow S.E. SiC RF sensor for continuous glucose monitoring. *MRS Advances (Electronics and Photonics)*. 2016. **1**, No 55. P. 3391–3696. https://doi.org/10.1557/adv.2016.400.
12. Chen F., Li G., Zhao E.R. *et al*. Cellular toxicity of silicon carbide nanomaterials as a function of morphology. *Biomaterials*. 2018. **179**. P. 60–70. https://doi.org/10.1016/j.biomaterials.2018.06.027.
13. Saddow S.E. *Silicon Carbide Biotechnology: A Biocompatible Semiconductor for Advanced Biomedical Devices and Applications*. Elsevier, 2016.
14. Beke D., Szekrényes Z., Czigány Z. Kamarás K. and Gali A. Dominant luminescence is not due to quantum confinement in molecular-sized silicon carbide nanocrystals. *Nanoscale*. 2015. **7**. P. 10982–10988. https://doi.org/10.1039/C5NR01204J.
15. Verma A., Krishna P. *Polymorphism and Polytypism in Crystals*. John Willey, 1966.
16. Kleber W. *An Introduction to Crystallography*. Berlin: Veb-Verlag Technik, 1971.
17. Adachi S. *Properties of Group-IV, III-V and II-VI Semiconductors*. John Willey, 2005. P. 4–21.
18. Chen S., Li W., Li X., Yang W. One-dimensional SiC nanostructures: Designed growth, properties, and applications. *Progress in Materials Science*. 2019. **104**. P. 138–214. https://doi.org/10.1016/j.pmatsci.2019.04.004.
19. Izhevskyi V.A., Genova L.A., Bressiani J.C., Bressiani A.H. Review article: silicon carbide. Structure, properties and processing. *Ceramica*. 2000. **46**, No. 297. P. 4–13. https://doi.org/10.1590/S0366-69132000000100002.
20. Vlaskina S.I., Mishinova G.N., Vlaskin V.I., Rodionov V.E., Svechnikov G.S. 8H-, 10H-, 14H-SiC formation in 6H-3C silicon carbide phase transitions. *Semiconductor Physics, Quantum Electronics and Optoelectronics*. 2013. **16**, No 3. P. 273–279. https://doi.org/10.15407/spqeo16.03.273.
21. Choyke W.J., Matsunami H., Pensl G. *Silicon Carbide: Recent Major Advances Technology & Engineering*. Springer, 2013.
22. Matsunami H. Fundamental research on semiconductor SiC and its applications to power electronics. *Proc. Japan. Academy Series B. Phys. and Biolog. Sci*. 2020. **96**, No 7. P. 235–254. https://doi.org/10.2183/pjab.96.018.
23. Vlaskina S.I., Mishinova G.N., Vlaskin V.I. Rodionov V.E., Svechnikov G.S. Peculiarities of photoluminescence spectra behavior in SiC crystals and films during phase transformations. *Semiconductor Physics, Quantum Electronics and Optoelectronics*. 2016. **19**, No 1. P. 62–66. https://doi.org/10.15407/spqeo19.01.062.
24. Ibrahim R.K.R., Yonus M.H., Khalajabadi S.Z., Abu A.B.H., Ameen O.F., Ahmad N., Redzuan N. Synthesis and characterization of nanocrystalline silicon carbide thin films on multimode fiber optic by means 150 MHz VHF-PECVD. *Int. J. Biosen. Bioelectron*. 2018. **4**, No 1. P. 0093. https://doi.org/10.15406/ijbsbe.2018.04.00093.
25. Smertenko P., Fenenko L., Brehmer L. and Schrader S. Differential approach to the study of integral characteristics in polymer films. *Advances in Colloid and Interface Science*. 2005. **116**, No 1-3. P. 255–261. https://doi.org/10.1016/j.cis.2005.05.005.
26. Luka G., Kopalko K., Lusakowska E., Nittler L., Lisowski W., Sobczak J.W., Jablonski A., Smertenko P.S. Charge injection in metal/organic/ metal structures with ZnO:Al/organic interface modified by $Zn_{1-x}Mg_xO$:Al layer. *Organic Electronics.* 2015. **25**. P. 135–142. https://doi.org/10.1016/j.orgel.2015.06.023.
27. Vlaskina S.I., Svechnikov G.S., Mishinova G.N. Vlaskin V.I., Rodionov V.E., Lytvynenko V.V. Nano silicon carbide's stacking faults, deep level's and grain boundary's defects. *Journal of Nano- and Electronic Physics*. 2018. **10**, No 5. P. 05021. https://doi.org/10.21272/jnep.10(5).05021.
28. Vlaskina S.I., Mishinova G.N., Vlaskin L.V., Rodionov V.E., Svechnikov G.S. Nanostructures in lightly doped silicon carbide crystals polytypic defects. *Semiconductor Physics, Quantum Electronics and Optoelectronics*. 2014. **17**, No 2. P. 155–159. https://doi.org/10.15407/spqeo17.02.155.
29. Osipyan Yu.A., Negryi V.D. Dislocation emission in CdS. *phys. status solidi.* 1979. **55**, No 2. P. 583–588. https://doi.org/10.1002/pssa.2210550227.

Authors and CV

Svetlana I. Vlaskina, Doctor of Sciences in Physics and Mathematics, 2004; PhD of Technical Sciences, 1982. Professor at the Yeoju University (Yeoju Institute of Technology), South Korea. Author of more than 80 scientific papers. Research interests: polytypism in wide bandgap semiconductors, phase transformations, deposition and growth technologies, optoelectronic devices, optical and electro-physical properties of semiconductors, bio-nano silicon carbide.

Galina N. Mishinova, Retired researcher at the Taras Shevchenko Kyiv National University. Author of more than 25 scientific papers. Research interests: optical properties of wide band semiconductors, polytypism, phase transformations, nano silicon carbide.

Ivan L. Shaginyan, Doctor of Dental Surgery (D.D.S.), Master of Science in Dental Science (M.D.S.), Department of Prosthodontics, Seoul National University, Dental College, Seoul, Korea. The research area in Dental Materials and Dental Occlusion.

George Svechnikov received the PhD degree in physics of semiconductors and dielectrics from the Institute of Semiconductors, Academy of Sciences of UkrSSR in 1981. Currently he is Associate Professor at the National Technical University of Ukraine "Igor Sikorsky Kyiv Polytechnic Institute". His research interests include ferroelectric materials, physics and devices in nanophotonics, ferro-electric materials, and quantum well optoelectronics. He has published more than 150 scientific papers. He is a Fellow of SPIE and Senior member of IEEE.

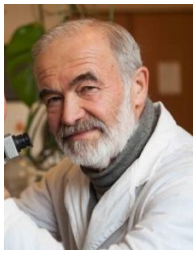

Petro S. Smertenko, defended his PhD thesis in Physics and Mathematics (Semiconductor Physics) in 1983. Senior researcher of Department of Optoelectronics at the V. Lashkaryov Institute of Semiconductor Physics, NAS of Ukraine. Authored over 150 publications, 30 patents, 8 textbooks. The area of his scientific interests includes physics and technology of semiconductor materials, hetero- and hybrid structures and devices (solar cells, photoresistors, light-emitting structures, *etc*.), as well as the analysis, diagnostics, modeling and forecasting of physical processes in various objects.

Характеристика нанобіокарбіду кремнію

С.І. Власкіна, Г.Н. Мішінова, І.Л. Шагінян, П.С. Смертенко, Г.С. Свєшніков

Анотація. Плазмове посилене хімічне осадження пари, реактивне магнетронне розпилення, хімічне осадження з гарячим дротом та посилене хімічне випаровування радіочастотною плазмою використовувались для розробки технології підготовки нанобіопокриття з карбіду кремнію з керамічних матеріалів для стоматологічних застосувань. Визнано вплив напруги зміщення, що застосовується до керамічних протезів та зубних коронок, на процеси кристалізації. Оптимальна напруга зміщення, яка подається на провідну підкладку, становила –200 В, тоді як для діелектричної основи напруга зміщення V_{bias} не впливала на властивості покриття SiC. Використовували аналіз вольт-амперних характеристик та спектроскопічну діагностику як методи вивчення механізму міжфазних перебудов для дослідження фазового переходу SiC у нанокристалічних покриттях з карбіду кремнію. Провідність покриття SiC збіглася з провідністю на діелектрику ($\mu n_0 = 10^{12}…10^{13}$ cm^{-1}·s^{-1}·V^{-1}). Провідна підкладка мала значний вплив на властивості покриття і це залежало від напруги зміщення V_{bias}. Провідність зросла на три-чотири порядки величини ($\mu n_0 = 3·10^{17}$ cm^{-1}·s^{-1}·V^{-1}), якщо напруга зміщення V_{bias} = –200 В. Збільшення напруги зміщення (V_{bias} = –600 В) призвело до зменшення провідності ($\mu n_0 = 10^{11}…10^{12}$ cm^{-1}·s^{-1}·V^{-1}). Встановлено, що в цій структурі існував режим подвійного введення з бімолекулярною рекомбінацією із залежністю $I = V^{3/2}$ для вольт-амперних характеристик SiC. Спектр люмінесценції покриття SiC на неділектричній кераміці (якщо V_{bias} = –200 В під час осадження) суттєво відрізнявся від спектра люмінесценції покриття SiC на діелектричній кераміці. Збільшення прикладеної напруги до підкладки V_{bias} під час осадження призвело до збільшення частки гексагональних політипів. Напрямки в кристалічній решітці за спектрами фотолюмінесценції були визначені із порівняння значень ширини нефононних частин розломів укладання та спектрів глибинного рівня в низькотемпературній фотолюмінесценції з розташуванням атомів у структурі решітки SiC. Зміщення кожного атома фотолюмінесценції, що брав участь, дозволило зробити кореляцію в технології осадження SiC та розробити технологію покриття SiC на стоматологічних матеріалах.

Ключові слова: карбід кремнію, карбід нанокремнію, кераміка на біологічній основі, вольт-амперна характеристика, фотолюмінесценція, стоматологічне застосування.